VI International Conference on Computational Methods in Marine Engineering
MARINE 2015
F. Salvatore, R. Broglia and R. Muscari (Eds)

MULTI-OBJECTIVE HULL-FORM OPTIMIZATION USING KRIGING ON NOISY COMPUTER EXPERIMENTS

Thomas P. Scholcz, Tomasz Gornicz and Christian Veldhuis

*Maritime Research Institute Netherlands (MARIN)
Haagsteeg 2, 6708 PM Wageningen, The Netherlands
e-mail: t.p.scholcz@marin.nl, web page: http://www.marin.nl

Key words: Hull-form optimization, multi-objective, meta-modelling, Pareto-front, cross-validation, Computational Fluid Dynamics, RANS

Abstract. Meta-modelling is a key technique for efficient multi-objective optimization in ship design projects using CFD. However, objective functions computed with CFD are not deterministic functions but contain random scatter about a smooth trend. Kriging is a meta-model technique that is well suited for numerical experiments with deterministic errors that can be perceived as random scatter due to varying input parameters. Simple Kriging, universal kriging and polynomial regression are used to obtain approximate Pareto-fronts from the hull-form optimization of a chemical tanker including free-surface effects. Cross-validation is used to assess the quality of the meta-models and the meta-model approximations of the Pareto-fronts are verified. It is found that cross-validation can be used to select the best meta-model but should not be used to estimate the true error of the approximation in case the design of experiment is too coarse. The approach is used in practice in order to accelerate the ship design process and to obtain more efficient ships with less vibration hindrance.

1 INTRODUCTION

Automatic optimization procedures based on CFD are becoming increasingly important in practical ship design. Building accurate high-dimensional meta-models of expensive computational codes is necessary for efficient optimization [1]. Objective functions obtained from CFD are not smooth, deterministic functions of the inputs but contain random scatter about a smooth trend. This numerical noise results from perturbations in the numerical solution of the physical phenomenon due to varying input parameters [2]. Numerical noise is an issue in any surrogate modeling approach [2, 3] and should be taken into account. In this contribution we demonstrate on a numerical example that:

- Cross-validation can be used in order to obtain reliable meta-models for the objective functions of interest.

- Multi-objective optimization on the meta-model yields an approximate pareto-front that - depending on the density of the sampling plan - gives a good indication of pareto-optimality.

1.1 CFD Solver

We use the viscous flow solver PARNASSOS [4], which has a solution technique that is very efficient with respect to both CPU-time and memory usage [5], which makes it very well suited for doing systematic variations or combination with an optimization strategy [6]. It computes the steady, turbulent flow around ship hulls by solving the discretised Reynolds-averaged Navier-Stokes (RANS) equations for steady, incompressible flow using a finite-difference method. Structured, HO-type body-fitted grids around the ship are used with a very strong contraction in wall-normal direction towards the hull in order to have y+-values below 1 near the wall, even for full-scale computations. Every RANS calculation includes a nominal (without propeller suction effect) and total (with propeller suction effect) calculation. The propeller action is modelled by means of a volume force field at the position of the propeller plane. In case of a hull-propeller optimization study multiple RANS calculations are performed. In that case the propeller force distribution over the propeller plane for all calculations is taken from one representative hull-propeller calculation in which the propeller is modelled by means of a Boundary Element Method (BEM).

1.2 Numerical test case

The above mentiod methods were used in the hull-form optimization process of a chemical tanker including free-surface effects. Especially when the stern shape is altered it is important to include free-surface effects, see [7]. The main particulars of the ship can be found in table 1. A CFD simulation was made for the original ship geometry at model scale. Based on these numerical results, 6 new hull shapes (variants) were proposed, see Figure 1 to 6. The changes with respect to the original hull-form are identified to overcome the particular hydrodynamic problems observed in the CFD results, as discussed in [7]. The new ship variants are described by design parameters ξ_j, with $j = 1, ..., 6$.

Table 1: Ship main parameters

Parameter	symbol	value	unit
Ship length	Lpp	166	$[m]$
Beam	B	31	$[m]$
Draught	T	10.8	$[m]$
Scale	λ	29.2	$[-]$
Froude number	Fn	0.207	$[-]$

1.3 Objectives

In the optimization process we are interested in the trade-off between the required power to propel the ship and the vibration hindrance due to the propeller loading and possible cavitation.

The required power is given by

$$P_D = \frac{R_T \times (1-w)}{1-t} \times \frac{V_s}{\eta_R \times \eta_0}, \tag{1}$$

where R_T is the towing resistance, w the estimated effective wake fraction, V_s the speed of the ship, t the thrust deduction coefficient, η_0 the propeller efficiency in open water and η_R the relative rotative efficiency. The latter is approximated by 1, while η_0 is obtained from the B-series of propellers [8] given a certain propeller wake field and thrust. The towing resistance follows from the nominal calculation. To compute the thrust deduction t, we also perform a second RANS computation (the total calculation) including a force distribution representing the propeller with an imposed thrust T_0 which is in the neighbourhood of the thrust T required for self propulsion. In such a way we can assume a linear behavior of the force on the hull as a function of the imposed thrust. The thrust deduction coefficient can then be computed from t=(R_0-R_T)/T_0, in which R_0 is the resistance force resulting from the second RANS computation. The effective wake fraction follows from the nominal wake fraction made effective by means of the force-field method, see [9]. With these quantities known we can calculate the hull efficiency η_H=(1-t)/(1-w).

The second optimization objective, vibration hindrance, is quantified by means of the so-called Wake Objective Function (WOF). The WOF should provide information on the quality of the wake field; small variations in angle of attack resulting in a smaller chance of vibration hindrance, and vice versa. Therefore we will use the L1-norm of the variation of the undisturbed propeller inflow angle

$$\beta = tan^{-1}\left(V_x / \left(\omega \frac{r}{R} - V_\theta\right)\right), \tag{2}$$

with V_x and V_θ the axial and tangential velocity components respectively, θ the angular position in radians and ω the propeller rotation rate in rad/s. The variation of β in circumferential direction as the propeller rotates is $\partial\beta/\partial\theta$. The L1-norm is determined from integration in circumferential direction and over a range of radii from the hub to the tip of the propeller:

$$WOF = \frac{\int_{R_{\text{hub}}}^{R_{\text{prop}}} \oint_\theta \left|\frac{\partial\beta}{\partial\theta}\right| f(\theta, r) d\theta r dr}{\int_{R_{\text{hub}}}^{R_{\text{prop}}} \oint_\theta f(\theta, r) d\theta r dr}, \tag{3}$$

Herein f is a weighting function that can be used to make the outer region and/or the top region of the propeller more important.

2 THEORY

2.1 Hull shape parametrization

Suppose that the hull shape is described by N control points d_i, $(i = 1, ..., N)$ of a B-spline surface. Furthermore, M interesting new shapes $d_{i,j}^{new}$, $(j = 1, ..., M)$ are identified by the hydrodynamic designer. A parameterized hull shape is then given by [10]

$$d_{i,j} = (1 - \xi_j) d_i^{\text{org}} + \xi_j d_{i,j}^{\text{new}} \quad (i = 1, ..., N \ ; \ j = 1, ..., M \ ; \ 0 \leq \xi_j \leq 1). \tag{4}$$

The hull shape is completely described by the parameters $\xi_1, ..., \xi_M$ in the M-dimensional unit hypercube which defines the design space. The advantage of this approach is that the designer can use his experience, skill and ingenuity to choose M hull shapes that are hydrodynamically relevant. The current test case uses 6 hydrodynamically relevant shapes, see Figure 1 to 6. These figures show the original ship (continuous lines) described by the B-spline control points d_i^{org} along with the new hull shapes (dashed lines) described by the control points $d_{i,j}^{\text{new}}$ with $j = 1, ..., 6$.

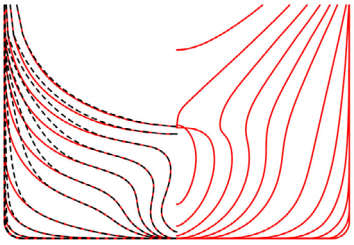

Figure 1: Variant 1 - straightening waterlines

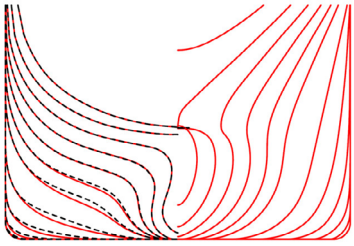

Figure 2: Variant 2 - straightening buttocks

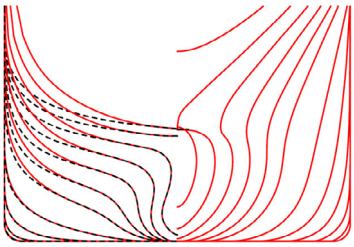

Figure 3: Variant 3 - widening transom

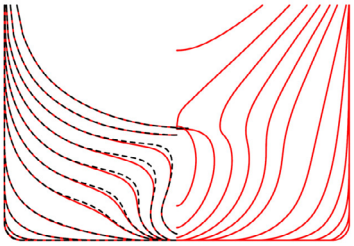

Figure 4: Variant 4 - gondola pronouncing

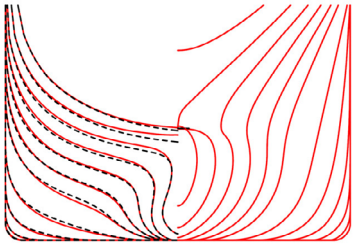

Figure 5: Variant 5 - changing buttock angle

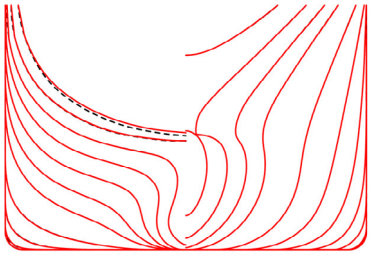

Figure 6: Variant 6 - changing transom immersion

2.2 Design of Experiment

We use a regular grid with nodes [0 0.5 1] in each dimension, resulting in $3^6 = 729$ CFD experiments. The grid is relatively course in order to limit the amount of CFD

calculations in the experiment. Adding one additional node for example would result in $4^6 - 3^6 = 3367$ additional CFD calculations: a tremendous increase. This effect is known as the curse of dimensionality which is a result of exponential scaling with the number of dimensions. Especially when the grid in the design space is course, it is important to check the quality of the constructed meta-model. This can be done using cross-validation.

2.3 Meta-model techniques

Meta-modelling has been identified as one of the key techniques to open the door for wider use of full-scale CFD applications by reducing the number of expensive CFD evaluations in optimization projects, see [11]. In this study we investigate three different meta-model methods: Polynomial regression, simple Kriging and universal Kriging. Polynomial regression is a parametric regression model which means that the model uses training points to estimate unknown parameters in the model. It is a well established method and easy to implement. The performance is best for a small number of design parameters ($m < 10$) and low-order non-linearity. Disadvantages are the risk of false optima due to oscillatory behavior and a large number of required training points, preferably on a regular grid. Kriging is a nonparametric interpolation model. Kriging imposes a global model that interpolates all design points and is well suited for numerical experiments with deterministic errors that can be perceived as random scatter due to varying input parameters. Moreover, the design space can be populated much more economical than the regular grid approach by using space-filling design of experiments like the Latin-Hypercube design or using the Sobol algorithm, see [12]. Due to this feature the method can be applied to problems with a large number of dimensions ($m < 50$) while still yielding accurate results. The main disadvantages of Kriging are the computational costs for model construction. A comparison between Kriging and polynomial regression is found in [13]. In the context of hull-form optimization, Kriging has been successfully applied in a number of design studies, see [12, 14, 15]. In section 2.3.1, 2.3.2 and 2.3.3 we will explain the meta-model techniques in more depth.

2.3.1 Polynomial regression

A polynomial model is assumed:

$$f(\boldsymbol{\xi}) = \alpha_0 + \sum_{i=1}^{k} \alpha_i \xi_i + \sum_{i=1}^{k} \sum_{j \leq 1}^{k} \alpha_{ij} \xi_i \xi_j + \text{ HOT}, \tag{5}$$

with α_i and α_{ij} the coefficients of the model and ξ_i the design parameters. Neglecting Higher Order Terms (HOT) in equation (5), a quadratic polynomial is obtained. The coefficients $\boldsymbol{\alpha}$ of the quadratic polynomial are obtained by solving the normal equations $\boldsymbol{\alpha} = \left[\mathbf{A}^T \mathbf{A}\right]^{-1} \mathbf{A}^T \boldsymbol{y}$, with $\boldsymbol{y}$ the observations and $\mathbf{A}$ the matrix of training points, see [13].

2.3.2 Simple Kriging

A Kriging meta-model is used [16, 17, 18], whose statistical foundation provides for natural treatment of noise in observations. In a Bayesian framework, the Kriging predictor is given by [19, 20]:

$$E(\boldsymbol{x}|\boldsymbol{y}) = \boldsymbol{\mu} + PH'(R + HPH')^{-1}(\boldsymbol{y} - H\boldsymbol{\mu}), \tag{6}$$

with quantity of interest $\boldsymbol{x}$, observations $\boldsymbol{y}$, drift $\boldsymbol{\mu}$, covariance matrix P, observation error covariance matrix R, and observation matrix H. The elements of the covariance matrix P are obtained from

$$p_{ij} = \sigma^2 \exp\left(-\sum_m \frac{h_{ij,m}^2}{2\theta_m^2}\right), \tag{7}$$

with lag $h_{ij} = |\xi_i - \xi_j|$, correlation range θ and dimensions of the parameter space m. Assuming independent observation errors, the observation error covariance matrix takes the form

$$R = \epsilon^2 \boldsymbol{I}, \tag{8}$$

where ϵ is the standard deviation of the noise which is estimated by maximizing the log likilihood, see [20]. When the drift $\boldsymbol{\mu}$ is assumed to be a known constant and the random process is assumed to be stationary, this method is called *simple Kriging*. Here, we choose the drift $\boldsymbol{\mu}$ equal to the mean of the observations $\boldsymbol{y}$.

2.3.3 Universal Kriging

In universal Kriging the drift or trend $\boldsymbol{\mu}$ in equation (6) is allowed to be non-constant and a function of the design variables, see [21]. The idea behind universal Kriging is that the model can be tuned regarding the trend in the data, hence giving better accuracy. Any prior knowledge on the response can be included in the drift. When a quadratic polynomial is used this method is called *Universal Kriging with quadratic drift*. In this contribution we use the quadratic polynomial from equation (5) to obtain $\boldsymbol{\mu} = \boldsymbol{\mu}(\boldsymbol{\xi}) = f(\boldsymbol{\xi})$.

2.4 Cross-validation

The root mean square error associated with the prediction of the meta-model in the design space is defined by

$$\mathrm{RMSE} = \sqrt{\int e^2(\boldsymbol{\xi}) d\boldsymbol{\xi}}, \tag{9}$$

where the integration is performed in the M-dimensional unit hypercube that defines the design space. The actual error is given by $e = y(\boldsymbol{\xi}) - \hat{y}(\boldsymbol{\xi})$, with y the actual value and

$\hat{y}$ the predicted value. Using a dense number of test points p_{test} filling this space, the integral in (9) can be approximated by

$$\text{RMSE}_{\text{approx}} = \sqrt{\frac{1}{p_{\text{test}}} \sum_{i=1}^{p_{\text{test}}} e_i^2}, \tag{10}$$

with the error $e_i = y_i - \hat{y}_i$ computed at the i-th test point. The RMSE in equation (10) is by definition more expensive to compute than the original Design of Experiment (DoE) and this is not desired from an industrial point of view. A practical solution to this problem is to use the one-leave-out cross-validation error instead. A cross-validation error is the error at a data point when the meta-model is constructed from a subset of the data not including that point.The cross-validation RMSE is defined by

$$\text{RMSE}_{\text{cross}} = \sqrt{\frac{1}{N} \sum_{i=1}^{N} e_{i,\text{cross}}^2}, \tag{11}$$

with N the number of experiments, $e_{i,cross} = y_i - \hat{y}_i^{N-1}$ the cross validation error and $\hat{y}_i^{N-1}$ the prediction from the meta-model that was constructed from the $N-1$ other points. The RMSE, approximated RMSE and cross-validation RMSE show often the same behaviour and are measures of the meta-model quality. For this reason, cross-validation can be used to obtain the best predictor in case of multiple meta-models, see [22].

2.5 Multi-objective optimization

When multiple objectives are considered in a design problem it is common to use the perspective of Pareto sets [21]. Members in a Pareto set of designs are all optimal in some sense, but the relative weighting between the competing goals - in this case the required power and the WOF - is not yet fixed. The designs in this set are *non-dominated* because no other design exceeds the performance in all goals. Although there are numerous advanced population based search algorithms (e.g. genetic algorithms), we use a basic population based search algorithm:

1. Evaluate the meta-model to obtain the predicted objective functions at a large number of uniformly distributed points in the design space.

2. Obtain a Pareto set using a non-dominated sorting algorithm on the list of objectives.

We use this algorithm since we do not aim to develop the most efficient multi-objective algorithm and since the evaluation of the meta-model is very cheap. It is possible to use the computed Pareto set to form an infill point set that - after running the full computions - can be used to refine the meta-model.

3 NUMERICAL EXPERIMENTS

3.1 Cross-validation

Cross-validation can be used for any meta-model technique but Kriging has the advantage of providing a standard deviation estimate at the i-th point in the cross-validation procedure. The estimated standard deviation from the Kriging model $\hat{\sigma}_i$ can now be compared to the cross-validation error at each point in the DoE. The number of standard errors that the actual value is above or below the prediction is given by [23]

$$\bar{e}_i = \frac{e_{i,cross}}{\hat{\sigma}_i} = \frac{y_i - \hat{y}_i}{\hat{\sigma}_i}, \tag{12}$$

which defines the standardized cross-validated residual at the i-th point. The Kriging model is valid when the values $\bar{e}_i$ are roughly in the interval $[-3\ 3]$ which is the 99.7% confidence interval in case of a Gaussian distribution, also known as the three-sigma rule. In case the distribution is not Gaussian, at least 98% should fall within the three sigma interval.

The cross-validation results for the required power are shown in Figure 7 to Figure 10. The actual values versus the predicted values are given in Figure 7 and Figure 9. The standardized cross-validated residuals are given in Figure 8 and Figure 10. Here, we compare the cross-validation results of simple Kriging with universal Kriging since polynomial regression does not provide standardized residuals. The performance of all meta-model methods is compared in Section 3.2.

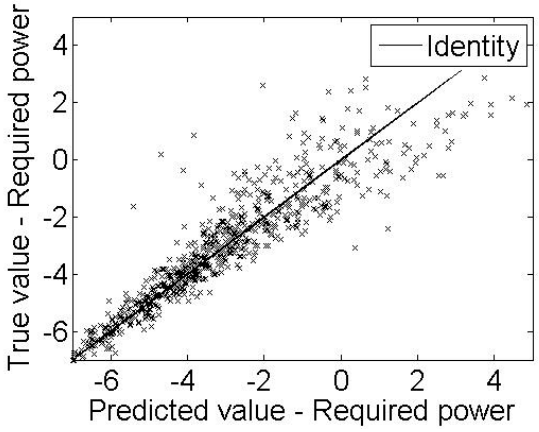

Figure 7: Simple Kriging: actual vs. predicted

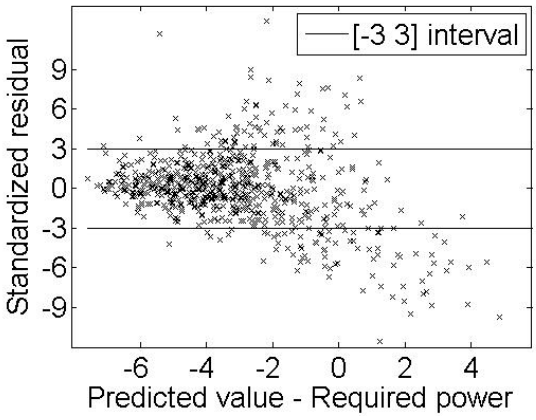

Figure 8: Simple Kriging: residuals $\bar{e}_i$

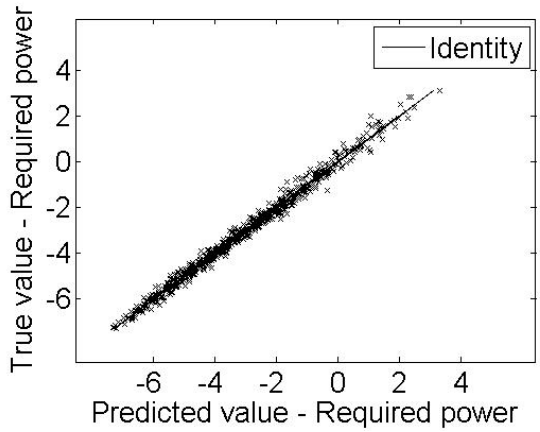

Figure 9: Universal Kriging: actual vs. predicted

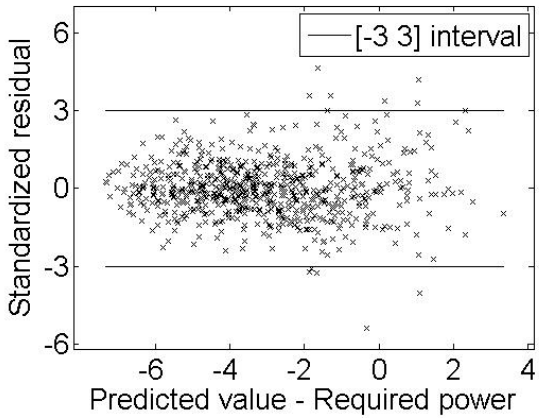

Figure 10: Universal Kriging: residuals $\bar{e}_i$

Simple Kriging yields a reasonable fit for low values of the required power but the accuracy breaks down for higher values. This can can be seen from Figure 7 which shows a larger distance to identity for higher values of the required power. From Figure 8 it becomes clear that the cross-validation errors do not always follow the three-sigma rule which means that the model is not valid in a global sense.

The actual values versus the Universal Kriging predictions in Figure 9 are much closer to identity than for Simple Kriging. Moreover, from Figure 10 we see that almost all standardized residuals obey the three-sigma rule.

Table 2: Comparison of cross-valdation results ($\text{RMSE}_{\text{cross}}$)

Method	Required Power	Wake Objective Function (WOF)
Simple Kriging	0.446	0.167
Universal Kriging	0.219	0.080

Table 2 summarizes the cross-validation results for the required power and the WOF. The cross-validation RMSE is much lower for Universal Kriging than for Simple Kriging . Here we see the advantage of including the trend of the data in the Kriging model.

3.2 Multi-objective optimization

The meta-model objectives are evaluated at $1 \cdot 10^7$ uniformly distributed points in the 6 dimensional designspace. The Pareto-front is then obtained by the use of a non-dominated sorting algorithm on the list of objectives. Figure 11 shows the Pareto-fronts obtained with polynomial regression, simple Kriging and universal Kriging together with the DoE.

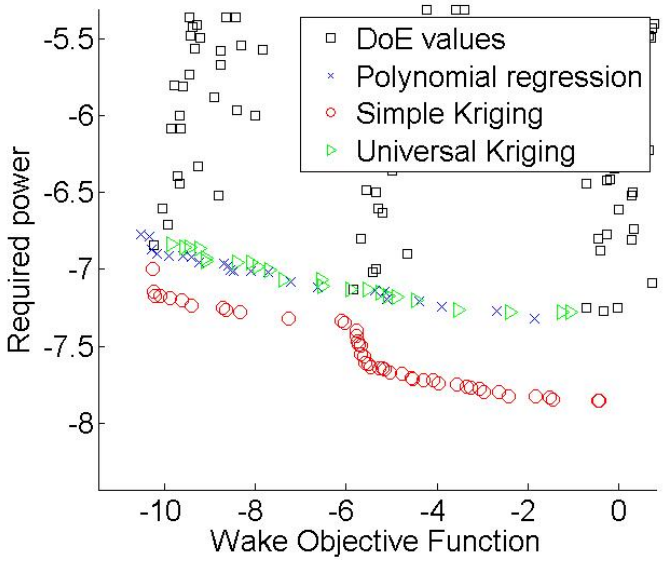

Figure 11: Design of Experiment and Pareto-front predictions

The simple Kriging predictions seem to underpredict the required power and the quadratic polynomial predictions seem to "overshoot" the DoE of the WOF. The accuracy of the Pareto points are verified by calculating the actual values of the objectives with Parnassos, see Figure 12 to Figure 15.

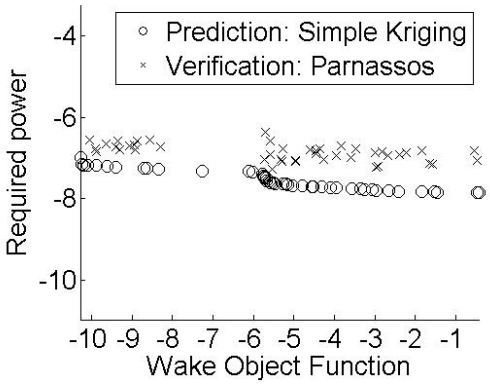

Figure 12: Verification - Simple Kriging

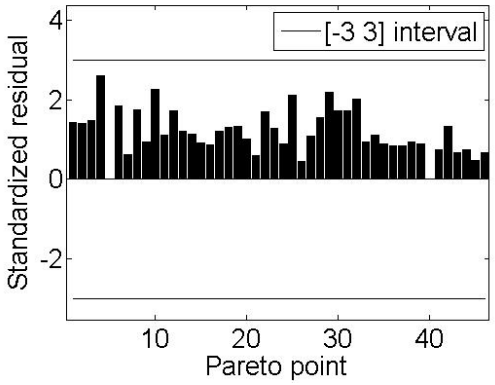

Figure 13: Standard error - Simple Kriging

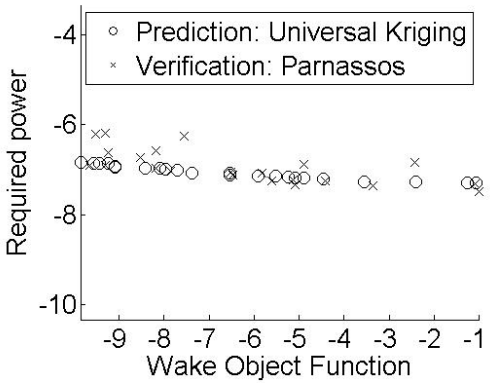

Figure 14: Verification - Universal Kriging

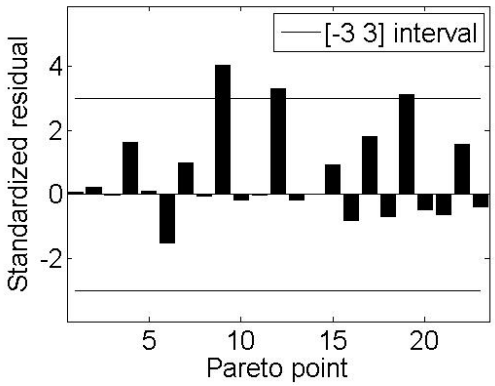

Figure 15: Standard Error - Universal Kriging

Figure 12 and Figure 14 show the predicted values and the verification values of the Pareto-fronts obtained with simple Kriging and universal Kriging respectively. Figure 13 and Figure 15 show the standard error based on the predicted standard deviation of both Kriging models. The simple Kriging predictions have a higher absolute error than the universal Kriging predictions. Moreover, the simple Kriging error is biased whereas the universal Kriging error is not. Both models are valid since the standard errors are in the interval $[-3\ 3]$. For simple Kriging this is due to the fact that the Pareto values are in a locally valid region of the model, see Figure 8.

Table 3 and Table 4 summarize the statistics of the error on the approximate Pareto-fronts for the required power and the WOF respectively.

Table 3: Error distribution - Required power

Method	Mean	Median	$\text{RMSE}_{\text{approx}}$
Simple Kriging	0.69	0.70	0.73
Polynomial regression	0.15	0.11	0.28
Universal Kriging	0.14	0.0069	0.37

From Table 3 we find that the universal Kriging method and the polynomial regression method of the required power are competing: universal Kriging has the lowest expected error and a smaller bias whereas polynomial regression has the lowest RMSE. For universal Kriging, the RMSE is high due to a few large errors at low values of the WOF, see Figure 14.

Table 4: Error distribution - WOF

Method	Mean	Median	$\text{RMSE}_{\text{approx}}$
Simple Kriging	0.11	0.27	2.13
Polynomial regression	0.18	0.15	2.03
Universal Kriging	-0.032	-0.0074	1.97

From Table 4 it becomes clear that universal Kriging performs best for the WOF. Although the error distributions are nicely centered at values close to zero we see that the $\text{RMSE}_{\text{approx}}$ of the WOF is much higher than the $\text{RMSE}_{\text{approx}}$ of the required power. However, from Table 2 we found that the cross-validation error of the WOF is much lower than for the required power. The reason can be found in Figure 11 where it can be seen that the density of the DoE is much coarser in the direction of the WOF than in the direction of the required power. The cross-validation error $\text{RMSE}_{\text{cross}}$ can be used to determine the best meta-model but cannot be used to estimate the approximate error $\text{RMSE}_{\text{approx}}$ since the number of test points p_{test} is much larger than the number of points in the DoE in this case. A possible way to improve the accuracy of the meta-model is to use the Pareto points as an infill point set by adding the points to the DoE.

4 CONCLUSIONS

Meta-modelling is a key technique to open the door for wider use of CFD applications in optimization projects for ship design. In order to obtain reliable meta-models, cross-validation can be used. Polynomial regression, simple Kriging and universal Kriging are investigated. Cross-validation indicates that universal Kriging performs better than simple Kriging. Verification of the multi-objective optimization results demonstrates that this is indeed the case. The cross-validation errors can be used to select the best meta-model but do not resemble the true errors of the meta-models when the DoE is too coarse. The meta-models could be refined by filling the DoE with points obtained from the optimization process in this case. This will be the subject of future research. However, the approach is already used to obtain approximate Pareto-fronts in practical ship design problems. It accelerates the ship design process and leads to more efficient ships with less vibration hindrance.

REFERENCES

[1] F. A. C. Viana, T. W. Simpson, V. Balabanov, and V. Toropov, "Metamodeling in multidisciplinary design optimization: How far have we really come?," *AIAA Journal*, vol. 52, no. 4, pp. 670–690, 2014.

[2] A. I. J. Forrester, A. J. Keane, and N. W. Bressloff, "Design and analysis of noisy computer experiments," *AIAA Journal*, vol. 44, pp. 2331–2339, 2006.

[3] A. I. J. Forrester, A. Sbester, and A. J. Keane, *Engineering Design via Surrogate Modelling, A Practical Guide*. Wiley, 2008.

[4] M. Hoekstra, *Numerical simulation of ship stern flows with a space-marching Navier Stokes method*. Technical University of Delft, 1999.

[5] A. van der Ploeg, M. Hoekstra, and L. Eca, "Combining accuracy and efficiency with robustness in ship stern flow computation," *Proceedings 23rd Symp. Naval Hydrodynamics, Val de Reuil, France*, 2000.

[6] A. van der Ploeg and H. Raven, "CFD-based optimisation for minimal power and wake field quality," *Proceedings 11th International Symposium on Practical Design of Ships and other Floating Structures, Rio de Janeiro*, pp. 92–101, 2010.

[7] A. van der Ploeg, "Rans-based optimization of the aft part of ships including free surface effects," *VI International Conference on Computational Methods in Marine Engineering*, 2015.

[8] G. Kuiper, "The Wageningen propeller series," *MARIN publication 92-001. Published on the occasion of its 60th anniversary.*, 1992.

[9] M. H. W. van Gent, "Force-field approach for propeller-wake interaction," *NSMB Report 44305-5-SR*, June1983.

[10] H. Raven and M. Hoekstra, "A practical system for hydrodynamic optimization of ship hull forms," in *VNSI Innovatiedag, Wageningen*, December 2003.

[11] K. Hochkirch and B. Mallol, "On the importance of full-scale CFD simulations for ships," in *12th International Conference on Computer and IT Applications in the Maritime Industries* (V. Bertram, ed.), pp. 85–95, April 2013.

[12] S. Harries, F. Tillig, M. Wilken, and G. Zaraphonitis, "An integrated approach for simulation in the early ship design of a tanker," in *10th International Conference on Computer and IT Applications in the Maritime Industries* (V. Bertram, ed.), pp. 206–220, May 2011.

[13] M. Ahmed and N. Qin, "Comparison of response surface and kriging surrogates in aerodynamic design optimization of hypersonic spiked blunt bodies," in *13th International Conference on Aerospace Science & Aviation Technology*, May 2009.

[14] H. Kim, S. Jeong, C. Yang, and F. Noblesse, "Hull form design exploration based on response surface method," in *Proceedings of the Twenty-first (2011) International Offshore and Polar Engineering Conference* (J. S. Chung, S. Y. Hong, I. Langen, and S. J. Prinsenberg, eds.), pp. 816–825, June 2011.

[15] G. Filip, D. H. Kim, S. Sahu, J. de Kat, and K. Maki, "Bulbous Bow Retrofit of a Container Ship Using an Open-Source Computational Fluid Dynamics (CFD) Toolbox," in *Proceedings of the SNAME Maritime convention*, October 2014.

[16] G. Matheron, "Principles of Geostatistics," *Economic Geology*, vol. 58, pp. 1246–1266, 1963.

[17] L. Gandin, *Objective analysis of meteorological fields: Gidrometeorologicheskoe Izdatel'stvo (GIMIZ), Leningrad*. Translated by Israel Program for Scientific Translations, Jerusalem, 1965.

[18] J. Sacks, W. J. Welch, T. Mitchell, and H. P. Wynn, "Design and analysis of computer experiments," *Statistical Science*, vol. 4, no. 4, pp. 409–435, 1989.

[19] C. K. Wikle and L. M. Berliner, "A Bayesian tutorial for data assimilation," *Physica D: Nonlinear Phenomena*, vol. 230, no. 1-2, pp. 1–16, 2007.

[20] J. H. S. de Baar, T. P. Scholcz, and R. P. Dwight, "Exploiting adjoint derivatives in high-dimensional metamodels," *AIAA*, vol. 53, no. 5, pp. 1391–1395, 2015.

[21] A. I. Forrester and A. J. Keane, "Recent advances in surrogate-based optimization," *Progress in Aerospace Sciences*, vol. 45, no. 13, pp. 50–79, 2009.

[22] F. A. Viana, R. T. Haftka, and S. Valder Jr., "Multiple surrogates: how cross-validation errors can help us to obtain the best predictor," *Structural and Multidisciplinary Optimization*, vol. 39, no. 4, pp. 439–457, 2009.

[23] D. Jones, M. Schonlau, and W. Welch, "Efficient global optimization of expensive black-box functions," *Journal of Global Optimization*, vol. 13, no. 4, pp. 455–492, 1998.